

Fakerat Software in the International Interferometric RadioAstron Project with Very Long Ground–Space Bases

V. I. Zhuravlev

*Astro Space Center of the Lebedev Physical Institute, Russian Academy of Sciences (FIAN ASC),
Leninskii pr. 53, Moscow 117924, Russia
e-mail: zhur@asc.rssi.ru*

Received December 16, 2013

Abstract—We present the description of Fakerat software developed for scheduling Very Long Baseline Interferometry (VLBI) observations on ground–space bases exceeding the size of the Earth. The results of scheduled observations using the Fakerat package, carried out during the first two years after launching the space radio telescope (SRT) in the space–ground interferometer mode, are reported in the paper.

DOI: 10.1134/S0010952515030090

INTRODUCTION

The RadioAstron space radio telescope (SRT) with a 10-meter reflector antenna onboard the “Navigator” base space platform was put into a high-elliptical orbit in July of 2011. The period of its revolution around the Earth was about 8.5 days. Detailed information on the spacecraft (SC) can be found in the RadioAstron User Handbook (2012) on the FIAN ASC website <http://www.asc.rssi.ru/radiastron/documents/rauh/en/rauh.pdf>, as well as in papers [1, 2]. In the first two years after SRT launching the tests of the space radio observatory have been performed according to the “Early Science Program (ESP) of the RadioAstron project.

At this stage, along with testing of the SRT onboard set of instruments, Fakerat software tests have been also performed. Fakerat software is designed for modeling the position of SRT pointed to the object, with regard to the design constraints on the SC orientation, the angle of SC visibility by the tracking ground station (TGS), as well as the angles of visibility of a source tracked by the ground-based radio telescopes. After modeling the decision was made on the possibility of performing interferometric sessions for each particular object taking into account its scientific objectives, the duration of observation, the observation date, the wavelength range, the interferometer base projection, the filling of *UV*-coverage, the tracking ground station¹ and ground-based radio telescopes.

¹ For data transmission in the interferometry mode at the ESP stage, only one high-informative radio channel (HIRC) of the tracking ground station was used, which was prepared in Pushchino on the RT-22 telescope basis. At the moment of paper writing, the second HIRC was prepared on the basis of the equatorial installation of the Green Bank 43-m radio telescope in the western hemisphere.

The Fakerat package is based on the programs contained in the “Caltech VLBI Analysis Program” package [3] and designed for scheduling and analysis of interferometric observations in the experiments with ground bases. Later on, in 1983, D.L. Meier (Jet Propulsion Laboratory) [4], while working on the “QUASAT” space project, added into the package the possibility of modeling the orbital radio telescope operation. The software has been further developed in D.W. Murphy’s work on the “VSOP” project [5, 6]. Murphy introduced into the package the constraints for the first “VSOP” space radio telescope specifically designed for interferometry, and added the graphical interface, which has provided customers with friendly support in the study of research perspectives of interferometric observations. This support greatly facilitated the work related to scheduling the experiment. Just at this stage of software development the Fakerat package appeared. Fakerat software was written in the Fortran language and implemented on SUN and HP working stations with the Unix operation system.

In the spring of 2011, six months before the RadioAstron launching, we have modified the Fakerat package with regard to the necessary constraints and some other features imposed on the SC in the RadioAstron project. The modification consisted primarily in full replacement of the orbital unit of the package. In the new orbital unit we took into account the disturbances of the RadioAstron orbital elements; we also introduced new functional constraints on the specified SC orientation, on the ground-based means of providing the RadioAstron functioning, and made some changes in the graphical interface for more convenient use of the software.

Currently, the modified version exists under the name Fakerat and is freely available on the FIAN ASC

Table 1

Date, time	x	y	z	v_x	v_y	v_z
	km			km/s		
Jun. 1, 2014 00.17.06:574	-110773.371	155550.653	-30793.986	0.435776	-1.292218	0.126814
Jun. 1, 2014 01.26.53:287	-108894.142	150064.383	-30247.683	0.462246	-1.328900	0.134241
Jun. 1, 2014 02.32.43:403	-107015.913	144743.696	-29702.761	0.489042	-1.365355	0.141747

website. Each user can acquire a compiled version of the Fakerat package along with the source code by the address: <http://www.asc.rssi.ru/radioastron/software/soft.html>. There one can also find the instructions for the Fakerat package installation on the IBM PC under the guidance of the Linux operation system, the package description, some techniques of working with the package, and some useful tips are given.

2. THE ORBITAL MOTION OF THE SPACECRAFT

The orbital motion of SC depends on the external forces acting on the vehicle. When considering the SC motion in the close vicinity of the Earth, i.e., at distances from a few hundred to thousands kilometers, the gravitational effect of other celestial bodies can be ignored [7]. However, when considering the SC motion at high altitudes, one should take into account the accelerations caused by the Moon and the Sun. The “VSOP” SRT orbit reached the altitude of 21400 km at the apogee and 560 km—at the perigee. The period of revolution around the Earth was equal to 6.3 hours. According to the model accepted in the Fakerat, due to relatively low orbital altitudes, the “VSOP” SRT motion was calculated in the Newtonian central gravitational field as an undisturbed one.

The value of the orbital altitude at the apogee for the RadioAstron SRT, when it entered the orbit after launching, was more than 15 times higher, than the value of the orbital altitude at the apogee for the “VSOP” SRT. The apogee altitude of the RadioAstron orbit was equal to 333.5 thousand km, the perigee altitude was 578 km, and the period of revolution was 8.32 days. This distinction in the orbital parameters was motivated by a desire to obtain an ultra-high angular resolution of objects. Here, the decrease in the degree of filling the UV -coverage was supposed to be compensated by the orbit evolution under an effect of disturbance from the Moon and the Sun.

On the other hand, the RadioAstron motion is disturbed by some other factors as well. Even relatively small forces, acting over a long period of time, can noticeably affect the orbit. During the flight over the high-elliptic orbit the SC is affected by the complexity of the gravitational field configuration near the Earth, by the solar radiation pressure, by the aerodynamic forces arisen at SC passage through the atmosphere at altitudes up to 1000 km, etc. These disturbances sig-

nificantly affect the SC orbit; so, the determination of the RadioAstron orbital elements requires another approach, which differs from that of the “VSOP” project.

In the Fakerat model the motion over the elliptical orbit is specified by tabular values of coordinates x , y , z and components of the velocity vector v_x , v_y , v_z of the SC center of masses in the geocentric coordinate system. Coordinates and velocity vector components are attributed to some time instant t . As an example, Table 1 gives the values of these coordinates and velocities as a function of time. The geocentric coordinates and velocities for the orbit as functions of time are calculated at the Keldysh Institute of Applied Mathematics (IAM) of the Russian Academy of Sciences (RAS).

To obtain the response of the interferometer, it is necessary to have the maximum possible accuracy of determination of SC coordinates and velocities. This is a rather time-consuming task; so, as a rule, the orbit calculation for a correlator is limited by the duration of observations. The accuracy of the reconstructed orbit at data processing in a correlator is, for the position in space, not worse than ± 500 m, and for the velocity, not worse than ± 2 cm/s. More detailed information regarding the orbit reconstruction can be found in [2]. The requirements for the accuracy of orbital elements in the Fakerat package are one-and-a-half to two orders of magnitude lower. This makes it possible to predict the orbit 5 to 6 years in advance, which is especially important for scheduling the future observations.

Figure 1 presents the elements of the spatial motion of SC over the elliptical orbit: a is the semimajor axis of the orbit, e is the orbit eccentricity ($0 \leq e < 1$); i is the orbital inclination, i.e., the angle between the orbital plane and the equatorial plane; Ω is the ascending node longitude of the orbit; ω is the angle between the pericenter and the ascending node of the orbit; τ is the time of satellite passage through the pericenter of the orbit.

The calculated evolution of six orbital elements up to the middle of the year 2019 is shown in Fig. 2. It shows that, under an effect of disturbances, the semimajor axis changes from 170 up to 200 thousand km, the eccentricity, from 0.57 to 0.97, and the orbital inclination changes from 0.4° to 84° .

There exist also several derived parameters: $a(1 + e)$ is the apocenter of the orbit, $a(1 - e)$ is the pericenter of

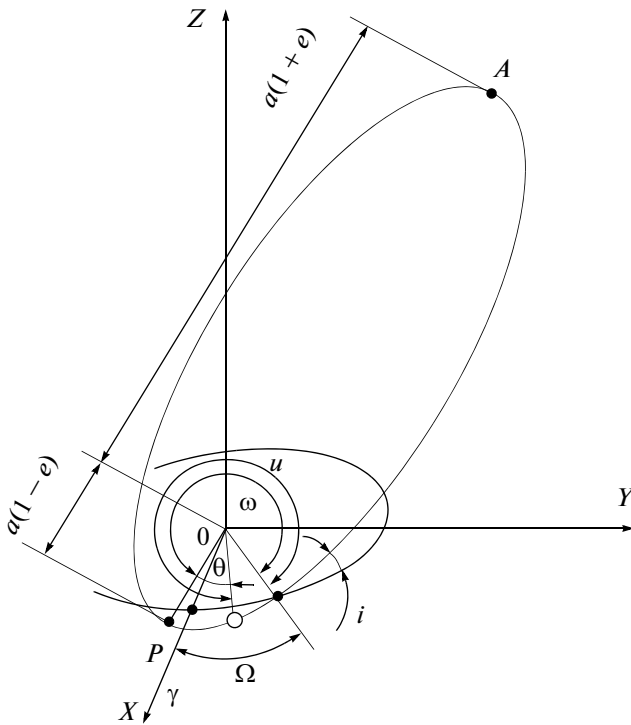


Fig. 1. The elements of the orbit is elliptical. γ is the ascending node of the orbit, A is the apocenter and P is the pericenter of the orbit.

the orbit, and P is the SC period of revolution (or the orbital period).

The SC orbital period is related with the size of the semimajor axis a as follows:

$$P = 2\pi(a^{3/2}/\sqrt{\mu}), \quad (1)$$

where $\mu = 3.9875 \cdot 10^5 \text{ km}^3\text{s}^{-2}$ is the coefficient equal to the product of the gravitational constant by the mass of the Earth. The quantity $\sqrt{\mu}/a^{3/2}$ is the mean angular velocity of SC motion over the orbit.

The change of the orbital period is associated with the change of the semimajor axis of the orbit, the orbital period being increased with growing semimajor axis. According to expression (1) and the calculated model of evolution of orbital elements, shown in Fig. 2, up to the year 2017 the orbital period will remain in the range from 8.3 to 9.2 days, and after 2017 the maximum value of the orbital period will increase up to 10.2 days.

On the other hand, the SC orbit is influenced by some disturbances, which are not determined a priori to a high accuracy. For example, these disturbances are associated with the action of reactive forces of the SC stabilization system's engines during unloading of gyroscopes. So, once every two to three months, on average, the IAM RAS provides the new updated tabular values of coordinates and velocities for the Fakerat. It is also important to update the orbit after its correction. So, for example, in late 2011, a few months

after SC launch, perigee altitude increased. Fortunately, such manipulations with SC happen rarely.

For Fakerat functioning it is necessary to know the values of SC coordinates and velocities at the intermediate time instants. To obtain these values, we approximate the orbit by an ellipse with Earth's center of gravity at one of ellipse's foci. Here we take into account that the values of quantities x, y, z, v_x, v_y, v_z at any point of the orbit are unambiguously related with the solution of Kepler's equations. Each new row of the table gives a new, updated approximation of the orbit. The semimajor axes of the ellipse, the ellipse orientation in space, as well as the SC localization in orbit were determined by six aforementioned elements. The plane of the orbit in space is specified by the orbit inclination and by the ascending node longitude. The pericenter of the orbit is determined by the angular distance from the ascending node to the orbit pericenter in the direction of SC motion. The time attribution is specified by the instant of SC passage through the pericenter. The pericenter determines the angular distance of an arbitrary point of the orbit: $u = \omega + \theta$, where θ is the true anomaly of this arbitrary point.

And, finally, the shape and size of the orbit are specified by the semimajor axis and eccentricity. The values of orbital elements largely determine the filling of the UV -coverage. Here, one should keep in mind that the highest angular resolution is achieved in the direction normal to the SRT orbit. The coordinates of normals (α, δ) for the northern and southern celestial hemispheres are defined by the following expressions: $(\Omega - 90^\circ, 90^\circ - i)$ and $(\Omega + 90^\circ, i - 90^\circ)$, respectively. In the RadioAstron project the monitoring of sources in the regions located near the normal to the orbit on the southern celestial hemisphere is rarely implemented due to functional constraints (see Section 3).

In Fig. 3 the normals to the orbit are designated as \textcircled{N} . In observations of radio sources in the areas close to the normal, the UV -coverage tracks are formed that have elliptic structure. This structure has large gaps. They will decrease when sources are moved from the normal to orbit projection in the celestial sphere. Their decrease is associated with simultaneous decrease of the angular resolution of a source. In the extreme case, when the source lies in the orbital plane, i.e., when it is located at the distance of 90° from the normal, the tracks of the UV -coverage form a linear structure. A more detailed description of Fig. 3 will be given below.

The sequence of operations at source observations, at adjusting and at laser location is determined by the Research program of works specified for the month ahead. This work is carried out by the operative SRT research group (FIAN ASC) [2]. The program takes into account scientific objectives, the current ballistic parameters of the orbit, the current constraints on the actuated ground-based radio telescopes and constraints

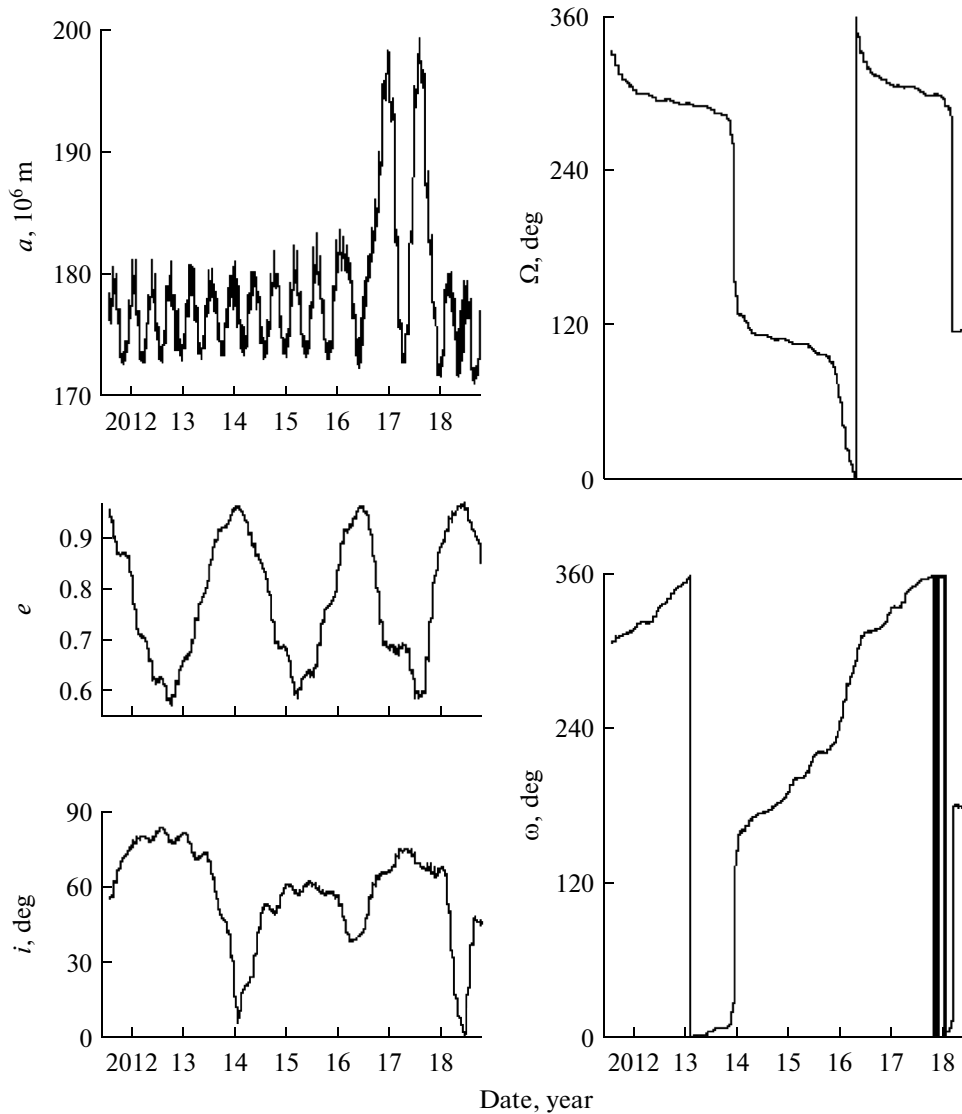


Fig. 2. Predicted values of changes of the orbital elements in time.

on the duration of observation modes for particular orientations of SC and positions of the HIRK antenna.

3. FUNCTIONAL CONSTRAINTS OF THE SPACECRAFT

There exist some constraints for the SC, which make it technically impossible for the SC to be pointing to any radio source, or make it impossible its effective monitoring. Below we describe only those constraints, which are incorporated in the Fakerat.

3.1. Constraints on the thermal regime. The observations cannot be performed: (1) if the angle between the SRT electric axis and the direction to the Sun center is less than 90° ; (2) if the angle between the SRT electric axis and the direction to the Sun center is larger than 165° ; (3) when the distance from the Earth center to the SC is less than 20 thousand km, and the

radio source is located at an angular distance from the Earth disc's center less than 30° .

3.2. Constraints for the power supply system. The angle between the direction to the Sun center and the normal to the plane of power supply system's panels should not exceed 10° .

3.3. Constraints for monitoring radio sources located closely from the edges of the Earth and the Moon. The observations cannot be performed when the radio source is located at the distance less than 5° from the closest edge of the Earth, and when the radio source is located at the distance less than 5° from the center of the disc of the Moon.

3.4. Constraints imposed on the star sensors. The onboard control complex includes three star sensors: AX1, AX2, and AX3. Only two of them operate in the normal mode. The axes of two sensors AX1 and AX2

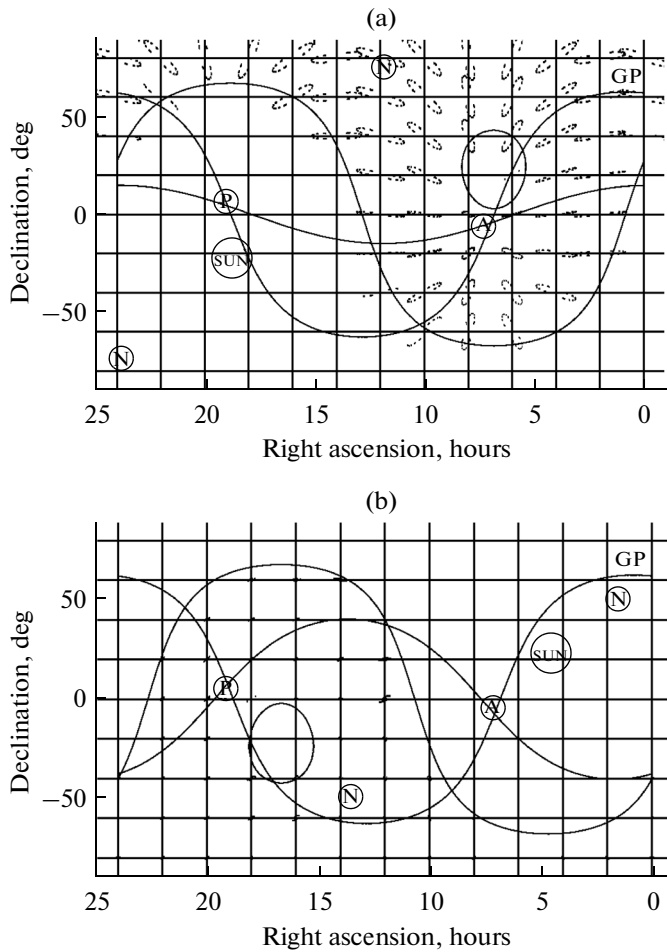


Fig. 3. Two examples of UV-coverage for the whole sky.

are located in the half-plane perpendicular to the electric axis X of the SRT and are turned around the axis parallel to the axis Y of rotation of the solar batteries' panel by the angle of 15° in the direction of axis $-X$, and at the angle of 45° to the axes Y and $-Y$, respectively. The axis of the third sensor AX3 is also located in the plane perpendicular to the SRT electric axis, but it is turned relative to axis $-X$ by 30° to the side of the third axis $-Z$. The coordinate system defined above is right-hand and orthogonal. According to the measurements performed by the Lavochkin Research and Production Association (Lavochkin RPA) in July 2012, the values of directing cosines of the star sensors are as follows:

AX1: $-0.86640913, -0.00055799, -0.499933447$

AX2: $-0.18425467, -0.70842875, -0.68130677$

AX3: $-0.18282000, 0.70791153, -0.68223024$.

The angle between the axis of each of two working sensors and interfering celestial body (the Sun, the Moon, and the Earth) must exceed the following: for the Sun, 40° (from the center of the Sun), for the Moon, 30° (from the center of the Moon), and for the Earth, 30° (from the nearest edge of the Earth).

3.5. Constraints for the high-gain communication antenna (HGCA) "Board-Ground". This antenna provides communication with the ground tracking antenna for transmitting the scientific and service information, and also provides frequency synchronization. The observation of a radio source is possible only when this communication really exists. The initial angular position of the HGCA drive relative to the base coordinate system of SRT, defined above, is specified by directing cosines:

axis X_n : $-0.95585102, -0.00818895, 0.29373758$

axis Y_n : $-0.00960202, 0.99994823, -0.00336890$

axis Z_n : $-0.29369479, -0.00604064, -0.95588015$.

The algorithm for calculating the angles of a drive of the HGCA for pointing its electrical axis to the science data receiving station is as follows. When calculating the angles ψ and ϑ it is necessary to take into account the angles δ_1 and δ_2 of the actual position of HGCA's electrical axis on the output flange of the HGCA drive.

For zero drive angles ($\psi = 0$ and $\vartheta = 0$) the angles δ_1 and δ_2 are determined as follows.

δ_1 —the angular deviation of the HGCA electric axis from the plane $X_n O_n Y_n$. The positive direction of measuring is performed to the side of the $-O_n Z_n$ axis.

δ_2 —the angular deviation of the HGCA electric axis projection on the plane $X_n O_n Y_n$ from the $O_n X_n$ axis. The positive direction is that to the side of the $O_n Y_n$ axis.

At the initial position $\delta_1 = 15.03^\circ$ and $\delta_2 = 0.32^\circ$.

For the unit radius-vector \mathbf{r} of the science data receiving station in the instrumental coordinate system the fulfillment of the following condition is checked:

$|\mathbf{r}_y| < \cos(\delta_1 + \delta_n)$, where δ_n is the value of a safety threshold. In the first approximation $\delta_n = 1^\circ$

The drive turning angles ψ and θ , under the assumption that $\delta_1 = 0$ and $\delta_2 = 0$, are as follows:

$$\begin{aligned} \psi &= \text{atan2}\left(-\mathbf{r}_z/\sqrt{1-\mathbf{r}_y^2}, \mathbf{r}_x/\sqrt{1-\mathbf{r}_y^2}\right) \\ &\quad - \arcsin\left(\sin \delta_1/\sqrt{1-\mathbf{r}_y^2}\right), \\ \vartheta &= \arcsin(\mathbf{r}_y/\cos \delta_1) - \delta_2. \end{aligned}$$

Then the values of calculated angles ψ and ϑ are checked for belonging to the working range:

$$\psi_{\min} \leq \psi \leq \psi_{\max}, \quad \vartheta_{\min} \leq \vartheta \leq \vartheta_{\max}.$$

The permissible range of turning angles is: for the angle ψ —from -73° to $+90^\circ$, for the angle ϑ —from -90° to $+90^\circ$. The positive direction of rotation of the HGCA drive is accepted to be defined by the right-hand coordinate system.

3.6. Constraints for the ground station of tracking and science data acquisition. The reception of research and service information in the RadioAstron project is performed on the ground-based 22-m radio telescope of the Pushchino Radio Astronomy Observatory (PRAO). The radio telescope should provide SRT tracking during the communication session. As men-

Table 2

GTS	X	Y	Z	dA/dt	dh/dt
	km			ang. min / s	
Pushchino RT-22	2916.9559	2248.6500	5190.0927	1.5	1.5
Green Bank	882.8799	-4924.4823	3944.1307	—	—

tioned above, currently it is possible to use the Green Bank tracking ground station there (TGS) with a mirror size of 43 m.

The geocentric coordinates and maximum rates of tracking in the azimuth dA/dt and in the elevation dh/dt of the TGS are listed in Table 2. The permissible range of TGS turning angles in Pushchino was updated in the course of performing the ESP: in the azimuth A it is from 6° to 354° , and in the height h it is from 10° to 84° . The permissible range of turning angles for the 43-m NRAO radio telescope is limited in the hour angle from -6.5 hour to 6.5 hour, and in the declination from -37° to 77° .

3.7. How does the sky area allowable for observations, change during a year? Figure 4 shows, in the (α, δ) coordinates, the celestial sphere's areas allowable for observations during one year. These areas are averaged with a step of one month in accordance with functional constraints for SC (given in this Section 3) and for the orbit (described in Section 2). The areas in Fig. 4, allowable for observations, are darkened. In order to get this picture, we have scanned the celestial sphere in the right ascension with a step of 30 min and in the declination with a step of 4° . In so doing, we have checked the possibility of performing SRT observation jointly with the ground-based radio telescopes, involved in the RadioAstron project, for each node of the grid. The signal accumulation time was not less than one hour.

As it is seen from Fig. 4, as the Sun moves from the southern hemisphere to the northern one, the area allowable for observations decreases. This is mainly due to the functional constraints, ensuring the normal thermal mode, and due to the possibility of HGCA pointing to the tracking ground antenna.

Another interesting phenomenon can be seen in Fig. 4. This is the motion of the areas allowable for observations to the side of increasing α during a year. Here, one may note that some particular sources can be observed at a certain time of the year only. The repeated observations are possible after a year only. Usually, the northern sources can be observed during 3 to 4 months within one year, and the southern ones, during 2 months or less.

4. THE FAKERAT PACKAGE USE STRATEGY

Currently the Fakerat with the graphical interface is running under the guidance of the Linux working

station in the X Window system. The Fakerat package shell is initiated after running the C Shell *run* script, which sets the medium of variables needed for running the libraries of the graphic PGPLOT package. If the package is set correctly, then the interactive menu of user interaction with the software from the Fakerat package should appear in the X Window. As mentioned above, the instruction for installing the package is located on the of the FIAN ASC site with the Fakerat software. Saving all introduced parameters via the graphical interface and transmitting them to the other programs is accomplished via the *menu_defaults* file, a copy of which is contained in the file *menu_defaults.1*. After the Fakerat start, a series of possibilities opens for the user for modeling the ground-space VLBI observations. As the work with the Fakerat has shown, at the ESP stage the most popular options occurred to be the following ones: (1) the review of the possibility of *UV*-coverage of the grid nodes ($\Delta\alpha = 2$ hours, $\Delta\delta = 20^\circ$) for the whole celestial sphere *all-sky uvplot*, (2) the time evolution of the *UV*-coverage for a particular chosen source *time-uvplot*, (3) the image of the *UV*-coverage of a particular source in an enlarged scale for a particular observation date *uvplot*, and (4) the test for violation of the constraints (see Section 3) when scheduling the observation *constraints*.

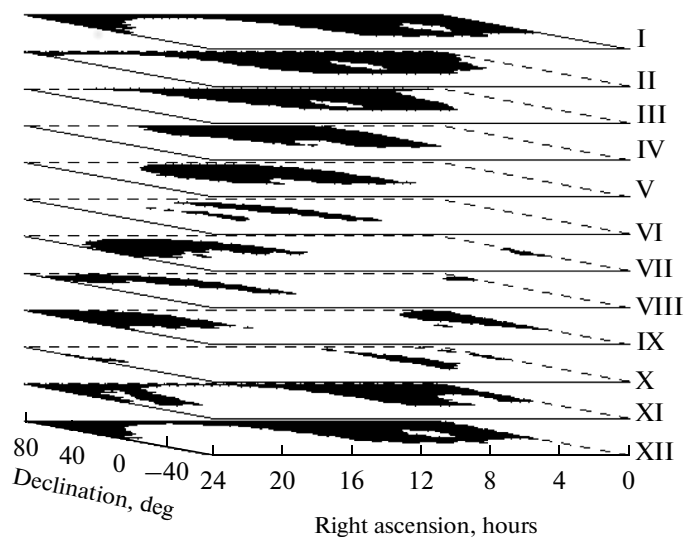


Fig. 4. The areas accessible (dark) and inaccessible (light) for observation.

The basic operations that must be accomplished before proceeding to modeling the *UV*-coverage are as follows:

to incorporate the orbit into the package; for this purpose in the *~fakera/orbit* directory of the deployed Fakera package, it is necessary to give a symbolic reference to the orbit with the name *ra_orbit*,

to select the tracking station for transmitting the *tracking station* data: PUSCHINO and/or GBANK-5,

to specify the observation date *obs-year, obs-month obs-day*,

to specify the observation starting time *star hh:mm:ss*,

to specify the observation stopping time *stop hh:mm:ss*,

to specify the receiver frequency *observing band*,

to specify the signal accumulation time $\tau(s)$,

to indicate the radio source *source name*,

to specify the angle of right ascension of a radio source *RA hh:mm:ss.ss*,

to specify the angle of declination of a radio source *Dec dd:mm:ss.ss*,

to choose ground-based radio telescopes intended to be used *telescopes*. We have already mentioned in Sections 2 and 3 some features occurring during the formation of the *UV*-coverage and which should be taken into consideration in scheduling the observations. At the beginning of work on a new source it is necessary, first of all, to determine the time interval when the observations are possible. This study can be performed with using two options: (1) *UV*-coverage of grid nodes throughout the celestial sphere, and (2) clarifying how the *UV*-coverage of a considered source changes with time. If the observation is impossible, then one can clear up the reasons of this by using the option called “the test for violation of the constraints.” Figure 3 shows, as a comparison, the typical *UV*-coverage of grids’ nodes for the whole celestial sphere for two opposite observation epochs: when the Sun is located in the southern part of the celestial sphere (the upper figure) and in the northern part of the celestial sphere (the lower figure). The *C* range (4.8 GHz) was used and the tracking station in Pushchino was running in this example. The following ground-based telescopes were used in this example: Arecibo, VLA27, GBT, Jodrell Bank, Evpatoria, Parkes, Kalyazin, Usuda, Noto, Shanghai, and Badary. The figure indicates the celestial sphere areas, which are inaccessible for observation due to constraints caused by the Sun. The projections of the Galaxy plane and SC orbital plane on the celestial sphere are presented. The apocenter, pericenter, and SC’s orbit normals are marked as (A), (P) and (N).

Again, it is clearly seen from the comparison of two *UV*-coverages, that in the summer period there exist considerable constraints caused both by the Sun, and by the possibilities of HGCA pointing to the tracking station.

Ground-based radio telescopes participating in ground–space VLBI experiments at the ESP stage, are listed in Table 3. The sensitivity of a pair of radio telescopes in the interferometric mode can be estimated as follows:

$$\sigma_{i,j} = 1/\zeta \sqrt{SEFD_i SEFD_j / 2B\tau},$$

where ζ is the coefficient of efficiency in relation to the non-quantized case. For the combination of levels with a single-bit clipped signal (the space-based radio telescope) and double-bit clipped signal (the ground-based radio telescope) $\zeta = 0.675$, and for the double-bit clipped signals (ground-based radio telescopes) $\zeta = 0.881$. Here it is assumed that signal recording was performed with the Nyquist frequency; $SEFD_{i,j}$ is the effective radiation flux density for the *i* and *j* radio telescope in Jy, respectively, τ is the signal accumulation time in sec and *B* is the receiver bandwidth in Hz. *SEFD* values are given in Table 3.

4.1. Frequency specification of the onboard complex of receivers. The RadioAstron carries the onboard complex consisting of four receivers, which allow the reception of a signal in four wavelength ranges. Each receiver (except the *C* band) has two independent channels, the inputs of which receive the signals possessing left (LCP) or right (RCP) circular polarization. In the *C* range (see below) the work with a single polarization only is possible. The band from the intermediate frequency (IF) output of receivers is formed in the Formator and equals 16 MHz for the upper (USB) and lower (LSB) bands. In the *P* range (see below) the signal transfer from the receiver output from the IF-range into the range of video frequencies is accomplished only for the upper or lower bands. Additional information on the functioning of the onboard research complex can be found in paper [2].

In each frequency channel the signal reception is possible in one of two central bands separated from each other by 8 MHz. The receivers provide signal reception:

in the *P* range with central frequencies of 308 or 316 MHz and radiometric path of 16 MHz; in the *L* band with the central frequencies of 1660 or 1668 MHz and radiometric path of 60 MHz; in the *C* range with central frequencies of 4828 or 4836 MHz and radiometric path of 110 MHz; in the *K* band with central frequencies of 22228 or 22236 MHz, with eight sub-ranges for a multi-frequency synthesis, with four sub-ranges for spectral observations of narrow radio lines and radiometric path of 150 MHz.

The central frequencies of the eight sub-ranges of the *K* range for a multi-frequency synthesis are separated from each other at 960 MHz: $F_{-4} = 18388$ or 18396 MHz, $F_{-3} = 19348$ or 19356 MHz, $F_{-2} = 20308$ or 20316 MHz, $F_{-1} = 21268$ or 21276 MHz, $F_0 = 22228$ or 22236 MHz, $F_1 = 23188$ or 23196 MHz, $F_2 = 24148$ or 24156 MHz and $F_3 = 25108$ or 25116 MHz.

Table 3. Ground-based radio telescopes and networks of radio telescopes in the RadioAstron project

Ground-based radio telescopes	Diameter	<i>SEFD</i>				Time
		<i>P</i>	<i>L</i>	<i>C</i>	<i>K</i>	
	m	Jy				%
EVN ^a :						
Arecibo (Ar)	305	12	3	2		11
Effelsberg (Eb/Ef)	100	600	19	20	90	51
Hartebeesthoek (Hh)	26		450	795	3000	6
Jodrell Bank (Jb1)	76	132	65	80		6
Jodrell Bank (Jb2)	25		320	320	910	2
Medicina (Mc)	32		700	170	700	31
Metsaehovi (Mh)	14				2608	3
Nanshan (Urumqi, Ur)	25		300	250	850	5
Noto (Nt)	32	980	784	260	800	29
Onsala (On)	25		320	600		5
Sheshan (Shanghai, Sh)	25		670	720	1700	4
Torun (Tr)	32		300	220	500	21
Westerbork (Wb)	14 × 25	150	40	60		26
Yebes (Ys)	40			160	200	50
Badary (Bd)	32		330	200	710	20
Svetloe (Sv)	32		360	250	710	20
Zelenchuk (Zc)	32		300	400	710	26
Robledo (Ro, DSS63)	70		35		83	17
LBA ^b :						
Narrabri, ATCA (At)	1 × 22		340	350	530	5
Ceduna (Cd)	30				2500	2
Hobart (Ho)	26		420		1800	5
Mopra (Mp)	22		340	350	900	2
Parkes (Pa)	64		42	110	810	2
Tidbinbilla (Ti, DSS43)	70		23		60	<1
VLBA ^c :						
VLBA_SC, VLBA_FD, VLBA_PT, VLBA_OV	25	2227	303	210	502	<1
ASKAP (Ak)	1 × 12		?			3
GBT ^d (Gb)	100	11	9	10	27	22
PT-70 (Ev)	70		19	19	110	47
Usuda (Us)	64		69	69	?	4
VLA27 ^e (Y)	1 × 25		420	310	560	<1
Warkworth (Ww)	12		?			3
Ooty (Oo)	530 × 30	?				<1
RadioAstron SRT	10	19000	3400	10500	30000	100

^a http://www.evlbi.org/user_guide/EVNstatus.txt^b http://www.atnf.csiro.au/vlbi/documentation/vlbi_antennas^c <http://science.nrao.edu/facilities/vlba/docs/manuals/oss2013b>^d <http://science.nrao.edu/facilities/gbt/proposing/GBTpg.pdf>^e <http://science.nrao.edu/facilities/vla/docs/manuals/oss2013a/performance/sensitivity>

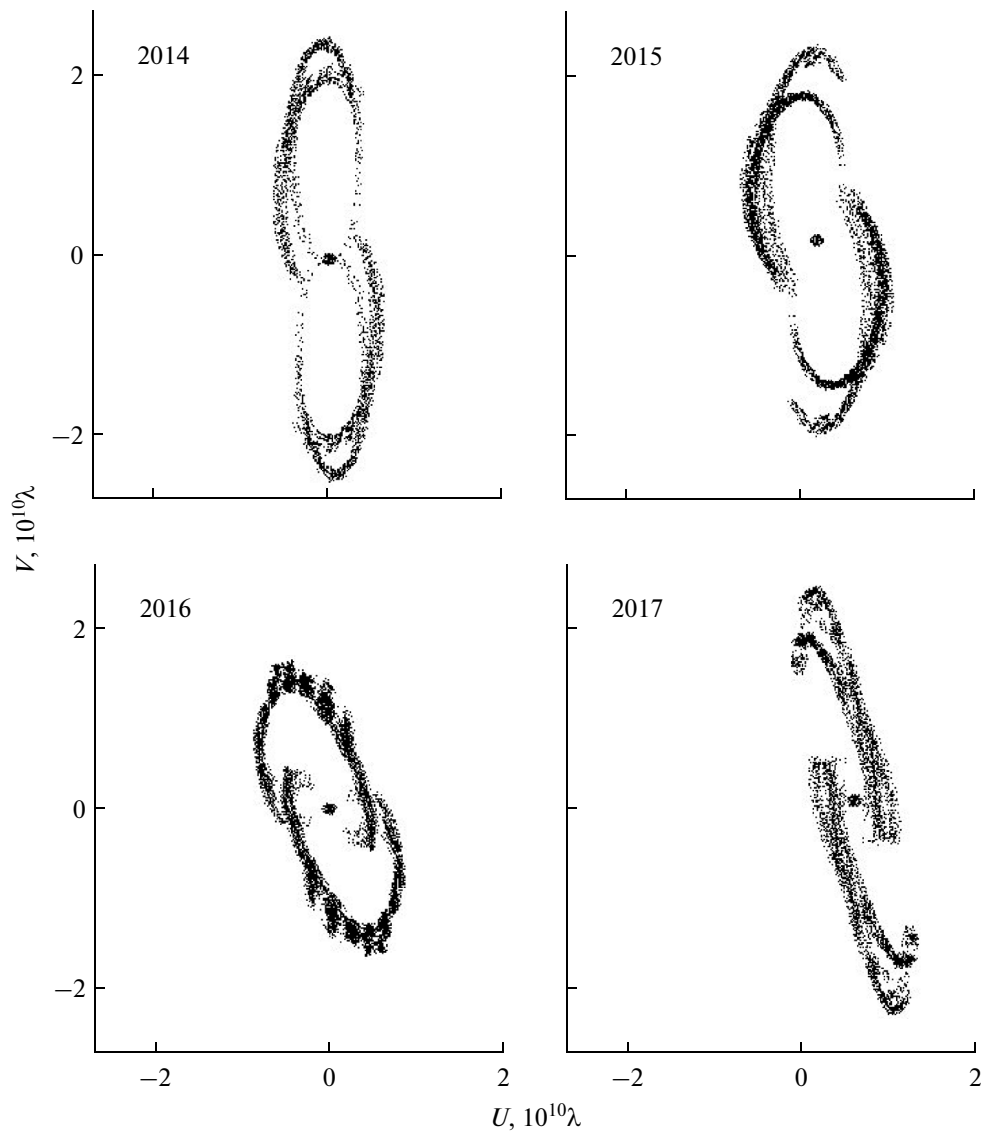


Fig. 5. Example of UV -coverage filling with tracks for the 0716 + 714 source.

The central frequencies of four sub-ranges of the K range for spectral observations of narrow radio lines are separated from each other at 32 MHz: $F_0 = 22228$ or 22236 MHz, $F_{0-1} = 22196$ or 22204 MHz, $F_{0-2} = 22164$ or 22172 MHz and $F_{0-3} = 22132$ or 22140 MHz.

The Fakerat package makes it possible to trace the filling of the UV -coverage of spatial frequencies by tracks in the process of synthesizing the image in the K range by means of eight sub-ranges from 1.19 to 1.63 cm. The process of filling of the UV -coverage by tracks for the 0716 + 714 radio source with using two extreme sub-ranges (1.19 and 1.63 cm) and eight ground-based radio telescopes (Effelsberg, GBT, Goldston, Jodrell Bank, Parkes, Robledo, Tidbinbilla and Eypatoria) from 2013 to 2015 inclusively is demonstrated in Fig. 5. The essential ellipticity of observed

coverages can be decreased in the future due to orbit correction.

CONCLUSION

By the end of Jun 2013, the FIAN ASC has scheduled and successfully accomplished about 650 interferometric sessions in all wavelength ranges accessible to the RadioAstron, with the participation of many largest ground-based radio telescopes and networks of radio telescopes EVN, LBA, and VLBA. All scheduling works were done using Fakerat software, including the earliest observations, whose program included observation of the Moon. When scheduling the Moon observations some functional constraints on SC in the Fakerat package were lifted. The total time of scientific observations by the end of June 2013 was more than 712 hours.

ACKNOWLEDGMENTS

The RadioAstron project is being implemented by the Astro Space Center of the Lebedev Physical Institute of the Russian Academy of Sciences and by the Lavochkin SPA under the contract with the Russian Space Agency in collaboration with many scientific and technological organizations in Russia and in other countries. The author considers it his duty to express gratitude to the Russian and foreign colleagues who participated in the Fakerat package elaboration:

to A.B. Alakoz, M.V. Popov and V.A. Soglasnyi for testing the package in the online mode when preparing the tasks for scheduling observations of galactic objects—pulsars and masers; to K.V. Sokolovskiy for testing the package in the automatic mode when preparing the tasks for scheduling observations of extragalactic sources—quasars and galaxies, as well as for developing the script making it possible to use the Fakerat package in the automatic mode, when the task for a package is sent via the data file without using the graphic interface window; to Yu.Yu. Kovalev for developing the network environment and for the package dislocation in the Internet on the Lavochkin SPA server;

to E.V. Kravchenko and J.M. Anderson (Max Planck Institute of Radio Astronomy, Bonn, Germany) for revision of the archive of ground-based radio telescopes;

to P.A. Voytsik and C.R. Gwinn (University of California, Santa Barbara, California, USA) for transforming the package into the 64-bit version and its distribution among IBM PC and Apple family users;

to V.G. Promyslov for the Fakerat package transferring from the Unix operation system, placed on the SUN platform, into the Linux operation system of the IBM PC family;

to V.E. Yakimov for the package dislocation on the FIAN ASC website and to T.S. Fetisova (freelancer) for scientific editing the text of the paper.

The author expresses special thanks to D. Murphy (Jet Propulsion Laboratory, NASA, Pasadena, US) for his participation in the RadioAstron project. This participation contributed to production, within the shortest time, of efficiently operating software for scheduling observations in the international interferometric ground-space RadioAstron experiment.

REFERENCES

1. Avdeev, V.Yu., Alakoz, A.V., Aleksandrov, Yu.A., et al., “Radioastron” space mission. The first results, *Vestn. NPO im. S.A. Lavochkina*, 2012, vol. 3, no. 14, pp. 4–21.
2. Kardashev, N.S., Khartov, V.V., Abramov, V.V., et al., “RadioAstron” – A telescope with a size of 30000km: Main parameters and first observational results, *Astron. Rep.*, 2013, vol. 57, no. 3, pp. 153–194.
3. Pearson, T.J. and Readhead, A.C.S., Image formation by self-calibration in radio astronomy, *Ann. Rev. Astron. Astrophys.*, 1984, vol. 22, pp. 97–130.
4. Ames, H., Bolton, S., and Burke, B.F., et al., Quasat: Technical aspects of the proposed mission, *ESA Spec. Publ.*, 1984, vol. 213, pp. 27–99.
5. Murphy, D.W., Simulations of space VLBI, in *Radio Interferometry: Theory, Techniques, and Applications, Proc. of the 131st IAU Colloquium*, vol. 19 of *ASP Conference Series* (ASP: San Francisco), 1991, vol. 19, p. 107.
6. Murphy, D.W., VSOP-2 mission simulations using the JPL-developed Fakesat software, *36th COSPAR Scientific Assembly, Held 16–23 July 2006, Beijing, China*, p. 2496.
7. El’yasberg, P.E., *Vvedenie v teoriyu poleta iskusstvennykh sputnikov zemli* (Introduction to the theory of flight of the Earth’s satellites), Moscow: Knizhnyi dom Librokom, 2011.

Translated by Yu. Preobrazhensky